

Niche theory for within-host parasite dynamics: Analogies to food web modules via feedback loops

Ashwini Ramesh  | Spencer R. Hall

Department of Biology, Indiana University, Indiana, USA

Correspondence

Ashwini Ramesh, Department of Biology, Indiana University, Biology Building 239, 1001 E 3rd Street, IN 47405, USA.

Email: aramesh@iu.edu

Funding information

Division of Environmental Biology, Grant/Award Number: 1655656

Editor: Tim Wootton

Abstract

Why do parasites exhibit a wide dynamical range within their hosts? For instance, why does infecting dose either lead to infection or immune clearance? Why do some parasites exhibit boom-bust, oscillatory dynamics? What maintains parasite diversity, that is coinfection *v* single infection due to exclusion or priority effects? For insights on parasite dose, dynamics and diversity governing within-host infection, we turn to niche models. An omnivory food web model (IGP) blueprints one parasite competing with immune cells for host energy (PIE). Similarly, a competition model (keystone predation, KP) mirrors a new coinfection model (2PIE). We then drew analogies between models using feedback loops. The following three points arise: first, like in IGP, parasites oscillate when longer loops through parasites, immune cells and resource regulate parasite growth. Shorter, self-limitation loops (involving resources and enemies) stabilise those oscillations. Second, IGP can produce priority effects that resemble immune clearance. But, despite comparable loop structure, PIE cannot due to constraints imposed by production of immune cells. Third, despite somewhat different loop structure, KP and 2PIE share apparent and resource competition mechanisms that produce coexistence (coinfection) or priority effects of prey or parasites. Together, this mechanistic niche framework for within-host dynamics offers new perspective to improve individual health.

KEY WORDS

coexistence, coinfection, feedback loops, intraguild predation, inverse Jacobian matrices, keystone predation, priority effects, within-host competition

INTRODUCTION

Parasites can show a variety of dynamics within hosts. These within-host dynamics can significantly affect health of individual hosts (Figure 1a–c; Cressler et al., 2014; Bashey, 2015), potentially altering population-level disease outbreaks (Gorsich et al., 2018; Mideo et al., 2008). For instance, larger infecting doses of parasite can sometimes overwhelm immune clearance leading to infection, while smaller doses become cleared (Fellous & Koella, 2009; Merrill & Cáceres, 2018). The success of invasion and persistence of a parasite within a host determines its

infection status or even death (Figure 1b; Duneau et al., 2017). Once infected, the stability of within-host dynamics can further impact host health. For instance, gut parasites that exhibit boom-bust dynamics (oscillations) decrease foraging in bees, deteriorating host health (Figure 1a; Otterstatter & Thomson, 2006). Similarly, competing parasites can exhibit successful coinfection (i.e. within-host coexistence), priority effects, exclusion or clearance that determines fecundity or longevity of individuals (Figure 1c; de Roode et al., 2005; Devevey et al., 2015). These divergent within-host dynamics, when scaled up, can create more disease in some population, and less in others (Vogels

This is an open access article under the terms of the [Creative Commons Attribution](https://creativecommons.org/licenses/by/4.0/) License, which permits use, distribution and reproduction in any medium, provided the original work is properly cited.

© 2023 The Authors. *Ecology Letters* published by John Wiley & Sons Ltd.

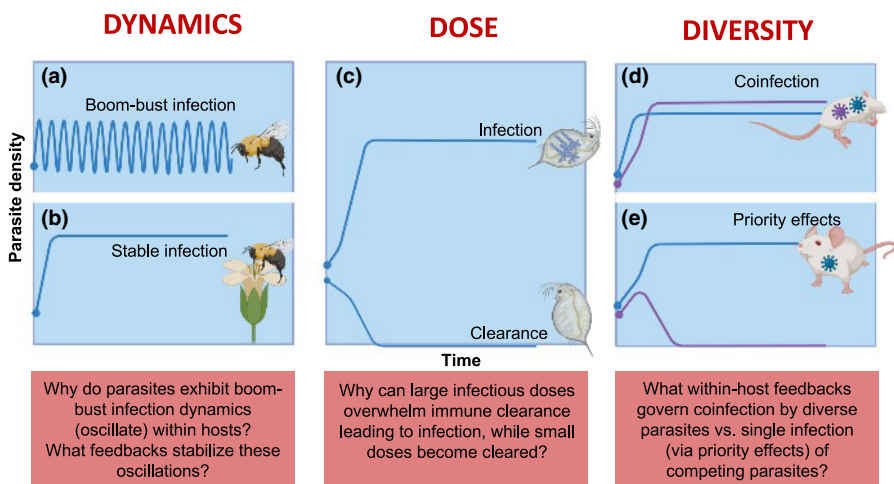


FIGURE 1 Unpacking infection dynamics using within-host ecological models: (a–e) Sample parasite densities over time capture how parasite dynamics, dose and diversity impact individual host health across various taxa (a, b) *Dynamics*: (a) Why do parasites exhibit boom-bust dynamics (oscillations)? (b) What within host and parasite factors stabilise these oscillations? (c) *Dose*: Why can large parasite doses overwhelm immune clearance leading to infection, while small doses become cleared? (d, e) *Diversity*: for competing parasites, what within-host feedbacks govern (d) coinfection versus (e) priority effects (where initial densities/order of arrival determines the winner). We address these questions using general principles outlined by within-host ecological models. See text for details. Figure created with [BioRender.com](https://biorender.com).

et al., 2019). Consequently, various dynamics of parasites can arise within hosts, likely mediated by immune systems and nutrient/energy availability (Cressler et al., 2014; Graham, 2008). While several mathematical models of within-host infection dynamics exist in the biomedical literature, they often describe specific model systems (Koelle et al., 2019; Pawelek et al., 2012). Yet, the broader fundamental puzzle remains: how do parasite dynamics, dose- and diversity link to individual health? What general principles govern those within-host dynamics?

Ecological models offer a powerful tool to outline general principles underlying infection dynamics. Here, we turn to two classic food web modules from community ecology for analogies. In intraguild predation (IGP), an omnivorous predator and its prey compete for a shared resource (Holt & Polis, 1997; Verdy & Amarasekare, 2010). Similarly, immune cells and a parasite compete for shared energy within a host (Figure 2a–c; Cressler et al., 2014). Hence, mechanisms that capture the repertoire of dynamics in IGP (stable coexistence, oscillations, priority effects, exclusion) might also produce those observed in single-parasite studies (Figure 1a,b). Additionally, in the diamond-keystone predation (KP) model, two prey species share a resource (exploitative competition) and a predator (apparent competition: Holt et al., 1994; Leibold, 1996). Similarly, two parasites can compete for a shared resource while facing immune attack (Figure 2d–f; first conceptualised here). In such a scenario, the KP model could anticipate the trade-offs and niche dimensions needed for coexistence, exclusion and priority effects of coinfecting parasites (Figure 1c). The underlying hope, then, is that food web modules might provide apt blueprints because they share basic consumer–resource

structure with their within-host analogues (Holt & Dobson, 2006; Lafferty et al., 2015).

However, a major complication arises: the enemy is generated differently in food webs versus within a host (Wodarz, 2006). Predators attack and assimilate prey for reproduction into new predators. Immune cells also attack parasites, but they simultaneously require host energy to produce new immune cells (Cressler et al., 2014). These ‘consumer–resource- like’ interactions imply that, mathematically, the immune production rate may depend on a product of immune cells, parasites and energy, whereas production of predators depends only the product of predator and prey abundance. Additionally, hosts can allocate a baseline level of energy straight to immune cells, a pipeline not enjoyed by even omnivorous predators in typical food webs. Therefore, these fundamentals of immune function—even when highly simplified—create more interaction links (Figure 2). Those additional links might alter feedbacks underpinning the range of stability outcomes (Metcalf et al., 2020). Hence, they might undermine analogies from food webs or create new outcomes altogether. Given these issues (Alizon & van Baalen, 2008; Fenton & Perkins, 2010), how could we compare and contrast stability in food webs (IGP, KP) to their within-host analogues?

We tackle this challenge by using a feedback loop approach. Feedback loops link the strength of consumer–resource interactions to stability (Puccia & Levins, 1991). Indeed, feedback loops characterise the biology behind stability and enable comparison of structurally similar but biologically distinct systems. Feedbacks can involve shorter, intraspecific direct effects (DE), where increases in intraspecific density leads to self-limitation (negative feedback) or facilitation (positive). However, longer

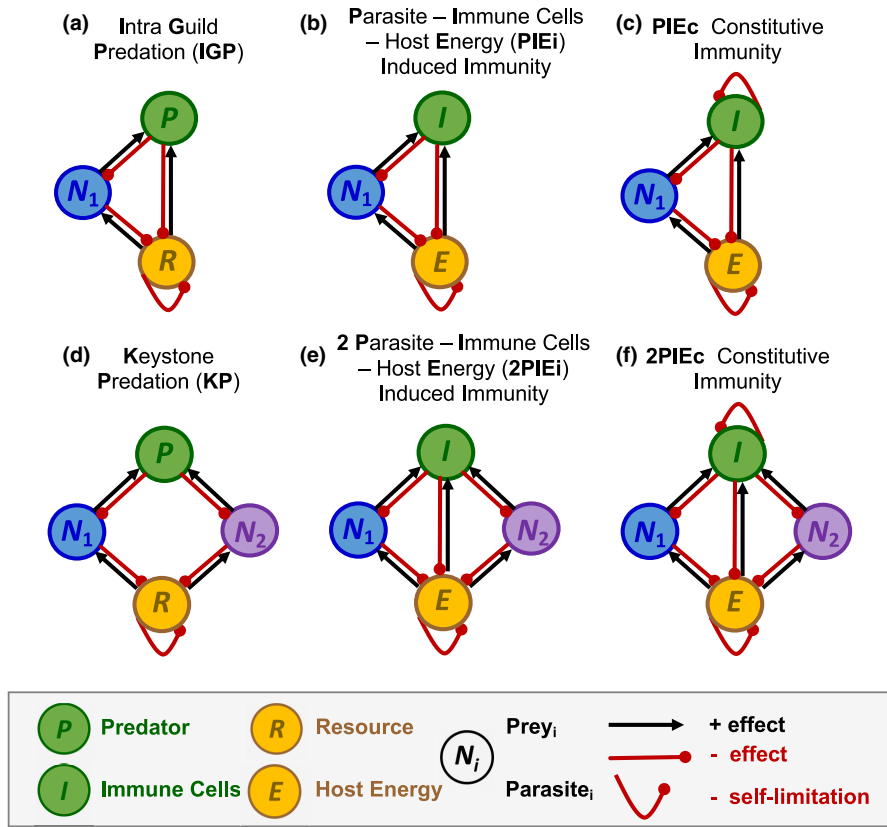


FIGURE 2 Direct interspecific effects and self-limitation in food web and within-host parasite models. *Top row*, single prey or parasite models (three-dimension, 3D): (a) one prey-predator-resource (intraguild predation, IGP), (b) one parasite-immune cells-host energy (PIEi) with induced immunity and (c) PIEc with constitutive immunity (i.e. fixed allocation of energy to production of immune cells). *Bottom row*, two prey or two parasite models (four dimension, 4D): (d) two prey-predator-resource (keystone predation, KP), (e) two parasite-immune cells-host energy with induced immunity (2PIEi), and (f) 2PIEc with constitutive immunity. All direct effects evaluated at positive densities (i.e. at a feasible interior equilibrium). Red (black) arrows: Negative (positive) interspecific direct effect; red curve: Negative intraspecific specific effect.

feedback loops arise, where each species interacts with others in longer chains of connected interactions—here, between two (e.g. binary consumer–resource), three or four species. As we describe, a subset of these longer chains of interactions for each species also lie at the heart of stability. We call these ‘intraspecific complementary effects’ (CE). As we then show, the sign and strength of lower and higher levels of feedback, translated into intra-specific direct and complementary effects, determines stability of the interactions.

Using intraspecific direct and complementary feedback loops, we first revisit the IGP and KP models. We then apply these loop-based lessons to analogous parasite–immune–energy models (PIE and 2PIE; Figure 2). We assume that parasite(s) respond to attack by a common immune system and share host energy (a resource). Additionally, we rely on local stability analyses of equilibria of deterministic ODE-based models (without stochastic effects, time delays, etc.). These assumptions oversimplify some examples (Ezenwa & Jolles, 2011), but they offer reasonable places to start (Graham, 2008; Griffiths et al., 2014). We then evaluate how host energy and immune system interact to mediate parasite dynamics within hosts (Figure 1a–c).

We aim to construct a mechanistic framework of within-host infection dynamics using analogies to classic food web modules. Hence, we conceptually unify free-living organisms in food webs and within-host infection entities. We do this using a traditional niche toolbox (trait trade-offs, bifurcations and assembly rules) and loop analysis. These tools empower synthetic comparison across structurally similar but biologically distinct systems. We ask three questions centred on parasite dynamics, dose and diversity (Figure 1a–c): (1) *Dynamics*: Why do parasites exhibit boom-bust infection dynamics (oscillate) within hosts? What feedbacks stabilise these oscillations? (2) *Dose*: Why can large infectious doses overwhelm immune clearance leading to infection, while small doses become cleared? (3) *Diversity*: What within-host feedbacks govern coinfection by diverse parasites versus single infection (via priority effects) of competing parasites?

Our results reveal the following. (1) Parasites oscillate when they more strongly regulate their growth rate via longer loops involving parasite, immune cells and resources than shorter, self-limitation loops. Those longer loops trigger delays that create oscillations while stronger self-limitation of resources and/

or immune cells stabilises them. (2) IGP predicts two types of priority effects. If they existed in the PIE models, they might explain why different doses lead to infection versus clearance. However, the nature of the generation of immune cells versus predators in IGP prevented such priority effects here. (3) Despite having simpler feedback links, KP anticipates the array of major coinfection outcomes. Specifically, competing parasites can exhibit symmetries (coinfection) or asymmetries (priority effects) in ratios describing ‘*effects on*’ their immune cells and energy versus how they are ‘*affected by*’ them. (4) Finally, allocation of energy to constitutive immunity enhances negative feedback, thereby shrinking regions of within-host oscillations, coinfection and parasite burden. Thus, feedback loops, guided by our interpretation schemes, show when and why comparable dynamics arise in these food webs and their within-host analogues. Together, this mechanistic niche framework for within-host dynamics offers new perspective to improve individual health.

METHODS AND RESULTS

Overview of the models

We compare and contrast modules of food web and within-host dynamics. The model with one prey, predator and resources (intraguild predation, IGP; Holt & Polis, 1997; Verdy & Amarasekare, 2010) parallels a within-host model of one parasite species, immune cells and host energy (PIE; modified from Hite & Cressler, 2018). Similarly, a two prey, predator, resource model (keystone predation, KP; Leibold, 1996) parallels one with a two parasite species, immune cells and host energy model (2PIE). However, while the food web and within-host modules share similar structure, they create enemies differently. Specifically, predators proliferate via direct consumption of their prey, while immune cells jointly require both parasites and a shared energy. Additionally, the within-host modules include two variants that commonly arise in host-parasite systems. In one, only parasites induce production of immune cells (PIEi and 2PIEi, induced immunity). In the other, energy is continuously allocated to maintain baseline immune function, even without parasites (PIEc and 2PIEc, constitutive immunity). Despite their differences, we compare across food web and within-host modules using feedback loops. Feedback loops provide a common metric to unpack the biology underlying stability. Jacobian matrices provide the starting point (Figure 3; Appendix Section 1 [hereafter: S1]). Each Jacobian term represents the direct effect of species j on growth rate of species i (J_{ij}), yielding (hereafter) interspecific *positive effects* (black arrow) and *negative effects* (red arrow) and intraspecific *self-limitation* (red curve) or *self-facilitation* (black curve;

Figures 2 [not seen here], 3). As shown below, these terms combine into loops at various levels.

One prey–predator–resource (IGP) | one parasite–immune cells – host energy (PIEi & PIEc)

At their heart, both IGP and PIE models hinge on binary consumer–resource-like interactions (Figure 2a–c, Table A1). In these interactions, consumers directly benefit while resources suffer direct costs. In IGP, omnivorous predators (P) can consume prey (N_1) and resources (R). An ‘interior’ equilibrium becomes feasible when each species can maintain positive density ($P^* > 0$, $N_1^* > 0$, $R^* > 0$). At IGP’s interior equilibrium, these consumer-resource interactions exert positive effects on the predator but negative ones on prey and resource. Then, prey also indirectly compete with predators for the shared resource. Consumption of resources benefits the prey and harms resources. Finally, chemostat-like renewal imposes self-limitation on resources (Figure 2a). Similarly, in the within-host models, immune cells (I) ‘consume’ two items, simultaneously killing parasites (N_1) while taking up host energy (E). At PIE’s interior equilibrium, these consumer-resource-like interactions have a positive effect on I and negative on N_1 and E . The parasite competes for this shared energy; its consumption positively affects parasites and negatively affects energy. Additionally, the donor-controlled renewal of host energy imposes self-limitation on energy without baseline allocation ($a_b = 0$, where a_b is baseline energy allocated to immune cells; Figure 2b). Fixed energy allocated to immune cells ($a_b > 0$) creates additional self-limitation on the immune cells in PIEc (Figure 2c).

Intraspecific direct and complementary effects: An approach using feedback (Figures 3 and 4, Figure A1)

To compare stability of these models, we used feedback loops (Figure 3). Any n -dimensional system can be decomposed into n levels of feedback that determine stability of an equilibrium (Figure 3, top panel). An interior equilibrium can allow stable or unstable coexistence (oscillations) or produce priority effects (if it is a saddle). As illustrated by and applied to IGP and PIE, the three-dimensional system creates three levels of feedback (Figures 3, 4; S1, S2). For example, level 1 feedback (F_1) is the sum of intraspecific direct effects (Figure 3) and is the Jacobian’s trace (S1). At the feasible interior equilibrium of IGP and PIEi (i.e. where all three variables have positive density), the basal resource/energy solely determines the relevant direct effects (Figure 4; S2). In these models, chemostat supply (dilution) and consumption of the resource both contribute to self-limitation, hence level 1

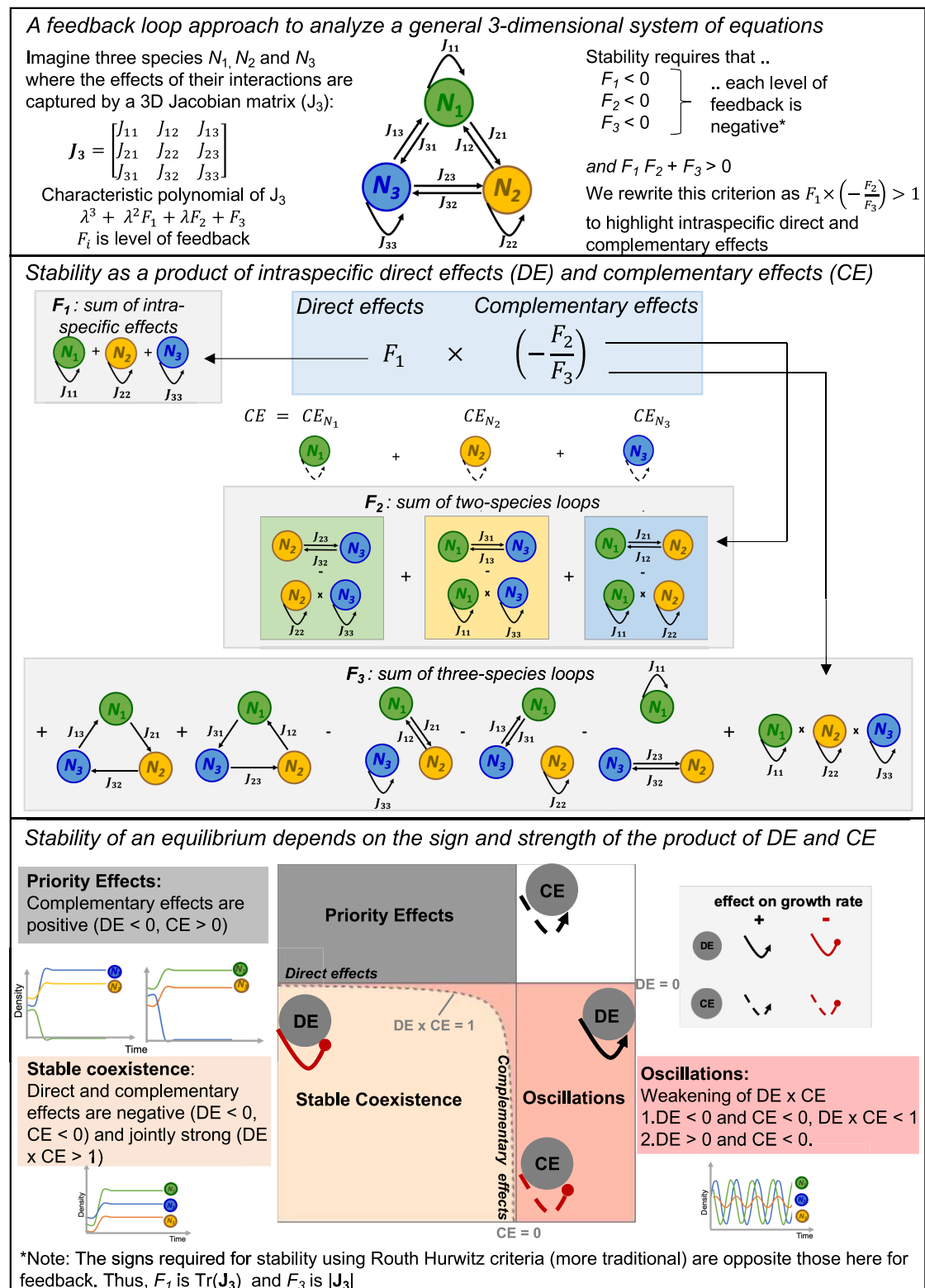


FIGURE 3 A feedback loop approach to analyse a general three-dimensional system of equations. *Top panel:* Stability analysis using Routh–Hurwitz criteria rearranged as three levels of feedback and a condition for oscillations ($F_1 F_2 + F_3 > 0$). *Centre panel:* Stability depends, in part, on the product of direct (DE) and complementary (CE) effects. DE or level 1 feedback (F_1) is the sum of single species loops. CE is a ratio of the longer loops, where each species interacts with other species in feedback at level 2 (F_2) and level 3 (F_3). It is also the sum of intraspecific complementary effects of each species (CE_{N_i}). The numerator of the intraspecific complementary effects of each species (CE_{N_i}) corresponds to specific combinations of the reciprocal two-species F_2 loops; the denominator for each species is F_3 (see S1). *Bottom panel:* The stability of an equilibrium depends on the sign and strength of the product of DE and CE producing either: stable coexistence (light orange), oscillations (dark orange) or a saddle (priority effects; dark grey). See offsets for details and sample dynamics.

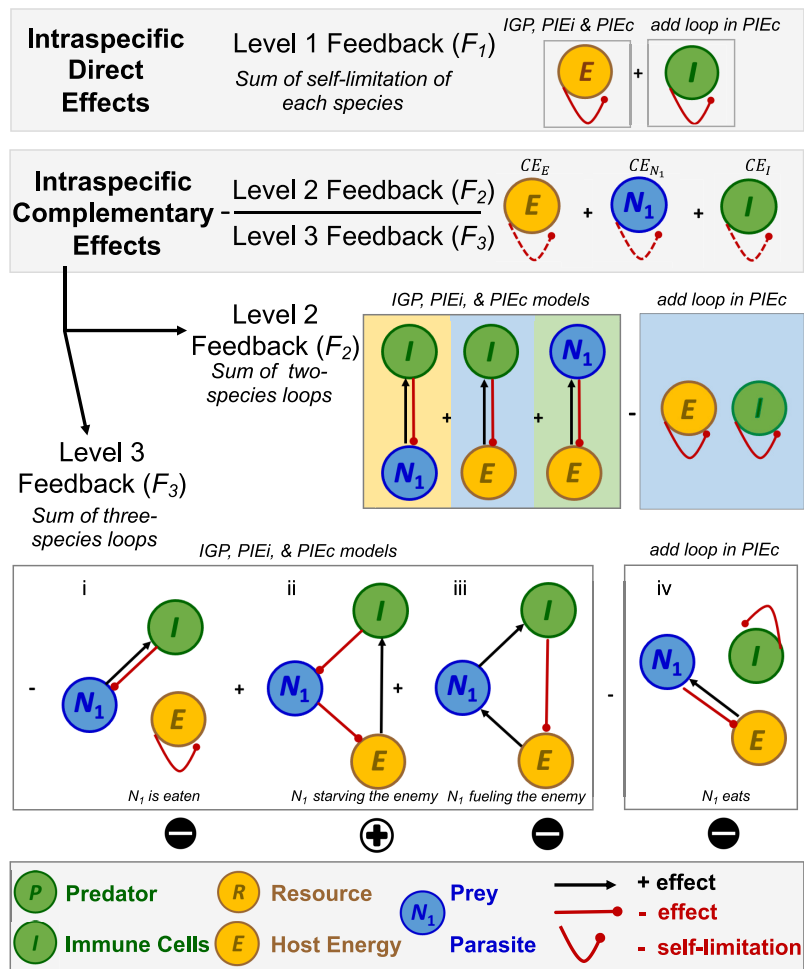


FIGURE 4 Intraspecific direct and complementary effects: An illustration of levels of feedback in IGP, PIEi and PIEc models (Figure 2a-c). Evaluated at a feasible interior equilibrium, the IGP and PIEi models have similar feedback structure. PIEc adds additional loops involving immune self-limitation. Level 1 feedback (F_1) is the sum of the shorter intraspecific direct effects (solid curves): self-limitation (-) of resource/energy and immune cells (PIEc only). In intraspecific complementary effects (dashed curves), each species limits or facilitates itself via interaction with other species in longer loops. The intraspecific complementary effect (CE) sums that of energy, E (CE_E ; yellow shading), parasite N_1 (CE_{N_1} ; blue) and immune cells I (CE_I ; green). CE, in turn, is a ratio of two levels of feedback. Level 2 feedback (F_2 , numerator of CE) sums pairwise consumer-resource loops (-) and the product of energy and immune self-limitation (-; only in PIEc; these are the numerators of the CE components). Level 3 feedback (F_3 , denominator of CE) sums three-species loops. These loops from L-R are: (i) ' N_1 is eaten', the $I-N_1$ loop times E self-limitation (-), (ii) ' N_1 starving the enemy' (+), (iii) ' N_1 fueling the enemy' (-) and (iv) ' N_1 eats', the $E-N_1$ loop times I self-limitation (-; PIEc only). This sum of (i)-(iv) determines the sign of F_3 and of CE (since $CE = -F_2/F_3$, and $F_2 < 0$ always). The predator (P, green), prey (N_1 , blue) and resources (R, yellow) in IGP are analogous to immune cells (I), parasite (N_1) and host energy (E), respectively, in the PIE models.

feedback (i.e. $F_1 = J_{RR} < 0$ and $F_1 = J_{EE} < 0$; see below). In PIEc, hosts also allocate baseline energy to immune cells ($a_b > 0$), thereby changing the interior equilibrium while adding self-limitation from immune cells (i.e. now $J_{II} < 0$, so, $F_1 = J_{EE} + J_{II} < 0$; S2).

Level 2 (F_2) feedback sums up two-species loops (Figure 3). In PIE models (Figure 4), F_2 sums three pairwise consumer-resource-like (+/-) interactions: growth of parasites after consumption of energy ($E-N_1$), growth of immune cells after consumption of that same energy ($E-I$) and killing of parasites by immune cells stimulating production of immune cells (N_1-I , with $R-N_1$, $R-P$ and N_1-P analogies in IGP respectively). At the interior equilibrium, all of these binary consumer-resource-like interactions add negative level 2 feedback (Equation A12.b,

A27.b). In PIEc, additional negative level 2 feedback comes from the product of energy and immune self-limitation. But, regardless of details, $F_2 < 0$ for all interior equilibria; hence, level 2 feedback stabilises.

Level 3 feedback (F_3) sums three-species loops. It is also the determinant of the Jacobian, $|J|$ (S1, S2). In PIE models, these loops at the interior equilibrium are (Figure 4, L-R): (i) ' N_1 is eaten', a negative loop coming from the stabilising product of the immune-parasite loop and energy self-limitation; (ii) ' N_1 starving the enemy', a positive loop where a small increase in the parasite reduces energy for the immune cells, hence reduces immune attack (i.e. $\uparrow N_1 \rightarrow \downarrow E \rightarrow \downarrow I \rightarrow \uparrow N_1$); (iii) ' N_1 fueling the enemy', a negative loop where a small increase of the parasite stimulates immune cells which consume energy

that then starves the parasite ($\uparrow N_1 \rightarrow \uparrow I \rightarrow \downarrow E \rightarrow \downarrow N_1$). Thus, negative feedback operates when N_1 hurts itself by ‘fueling’ the immune cells. Similar loops arise in IGP. Finally, in only PIEc, (iv) a negative ‘ N_1 eats’ loop arises from the stabilising product of energy consumption by the parasite and immune self-limitation.

Combined, these three levels of feedback determine stability of the interior equilibrium. First, stability requires that each level of feedback is negative (so, $F_1 < 0$, $F_2 < 0$, and $F_3 < 0$). When $F_3 < 0$, the interior equilibrium is stable; when $F_3 > 0$, it is a saddle. Additionally, stability requires that $F_1 F_2 + F_3 > 0$, or that upper level feedbacks (F_3) not be too strong relative to lower level feedback (F_1 , F_2). All of these conditions have analogies to the Routh-Hurwitz criteria, differing only in sign (Hurwitz, 1895; Puccia & Levins, 1991; Routh, 1877). Here, we also reframe stability analysis as sums of intraspecific direct effects (F_1 , hereafter DE) and of intraspecific complementary effects ($-F_2 / F_3$, the trace of the inverse Jacobian; CE; **S1**; **Figure 3**, top panel; **Figure A1**). Written this way, CE is a ratio of the longer loops, where each species interacts with other species in feedback at level 2 (F_2) and level 3 (F_3). It is also the sum of intraspecific complementary effects of each species N_i (lying on $\text{tr}[\mathbf{J}^{-1}]$; **Equation 1**; **Figure 3**, centre panel; **Figure A1**):

$$\text{CE} = \text{CE}_{N_1} + \text{CE}_{N_2} + \text{CE}_{N_3} = \sum \frac{-F_{2,N_i}}{F_3} = \frac{-F_2}{F_3} \quad (1)$$

The numerator of each species' intraspecific complementary effects (CE_{N_i}) is the subsystem feedback between the other two species [as detailed in **S1**]. The denominator for each species is level 3 feedback (**Equation 1**). For example, the complementary effect of N_1 , CE_{N_1} , is the N_2 - N_3 subsystem feedback, all divided by F_3 (green shading over grey shading, **Figure 3**, centre panel). Similar expressions can be derived for species 2 (CE_{N_2} , yellow shading) and 3 (CE_{N_3} , blue shading). We opt for a sign convention where CE that contribute to stability have negative sign (hence CE is the $\text{tr}[\mathbf{J}^{-1}]$ rather than $\text{tr}[-\mathbf{J}^{-1}]$; see **S1**). With DE and CE in hand, stability then depends on their sign and the strength of their product (**Figure 3**, bottom panel). Specifically, *stable coexistence* occurs when direct and complementary effects are negative (DE < 0 , CE < 0) and jointly strong (DE \times CE > 1 ; light orange). *Oscillations* arise when direct and complementary effects are jointly weak (DE \times CE < 1 for DE < 0 , or DE > 0 ; dark orange; equivalent to $F_1 F_2 < -F_3$). Finally, *priority effects* can occur with positive complementary effects (i.e. when CE > 0 ; for the models here, $F_2 < 0$ always, so CE > 0 implies $F_3 > 0$). The equilibrium experiencing positive feedback is a saddle (grey region). Note: priority effects (synonymous with alternative stable states) denote how initial densities, even offset in time (e.g. sequential infection), can determine competitive outcomes (depending on whose domain of attraction they move through).

Genesis or stabilisation of oscillations in IGP and PIE (**Figure 5, S2**)

Assembly of interior equilibria

To compare stability outcomes across IGP and PIE models, we created parallel 2D bifurcation diagrams (**Figure 5, S2**). These diagrams show stability outcomes across gradients in nutrient supply (S) and feeding rate of prey/parasite N_1 on the resource, f_{N_1} (**Figure 5a–c**; interpreted with 1D bifurcation diagrams: **Figure 5g–i**). The lines within the 2D bifurcation diagram represent shifts in species composition or in dynamics (stable coexistence, oscillations or priority effects; **S2** for full analysis). In IGP (**Figure 5a**), when nutrient supply and feeding rate of prey are too low to meet the minimal resource requirement (R^*) of either the prey or predator, only R is supported in the system (R , yellow). Increasing S allows R to meet the R^* of the predator (hence P invades, creating the R - P region [green]). As feeding rate of prey (f_{N_1}) increases along a fixed nutrient supply ($S = 110$), prey better compete for resources at the R - P boundary. Hence, the prey can invade; both prey and predator push R^* lower in the R - N_1 - P interior equilibrium (**Figures 5a, g**). In this region, R - N_1 - P coexist either stably (light orange) or via oscillations (dark orange). On the other hand, as the feeding rate of prey increases at low S ($S = 5$), prey invade the resource-only boundary (creating the R - N_1 region [blue]). The omnivorous predator can then invade this R - N_1 boundary creating stable coexistence (orange; **Figure 5a**). Thus, R , R - P , R - N_1 and R - N_1 - P equilibria (oscillatory and stable) are possible in IGP (**S2A**).

The within-host PIE model contains some but not all analogous states. The key differences stem from how hosts produce immune cells. In PIEi (**Figure 5b**), immune cells only generate with parasites. Hence, a host energy-immune (E - I) state, analogous to the R - P one, is not possible. Similar to IGP, low feeding rate can prevent parasite invasion (creating the E -only state [yellow]). With increasing feeding rates (illustrated at $S = 500$), parasites (N_1) can eventually invade, creating E - N_1 space (light blue; **Figure 5h**). Although parasites depress E^* , sufficiently high parasite density meets the immune system's minimal E N_1 requirement (**Figure 5h**). Hence, at medium to high feeding rates of parasites, E - N_1 - I coexist either stably (light orange) or via oscillations (dark orange). However, at sufficiently high f_{N_1} , parasites compete too strongly: they successfully starve out the immune cells, re-establishing a E - N_1 space (blue). Thus, PIEi exhibits only three equilibria: E , E - N_1 and E - N_1 - I (oscillations and stable coexistence; **Figure 5b**; refer **S2B**).

In PIEc, the host always allocates energy to the immune system ($a_b > 0$). This biology eliminates the E -alone and E - N_1 region. Instead, immune cells prevent infection (E - I space; low f_{N_1} ; green) or hosts become infected (E - N_1 - I space; higher f_{N_1} ; orange). Like IGP, at high feeding

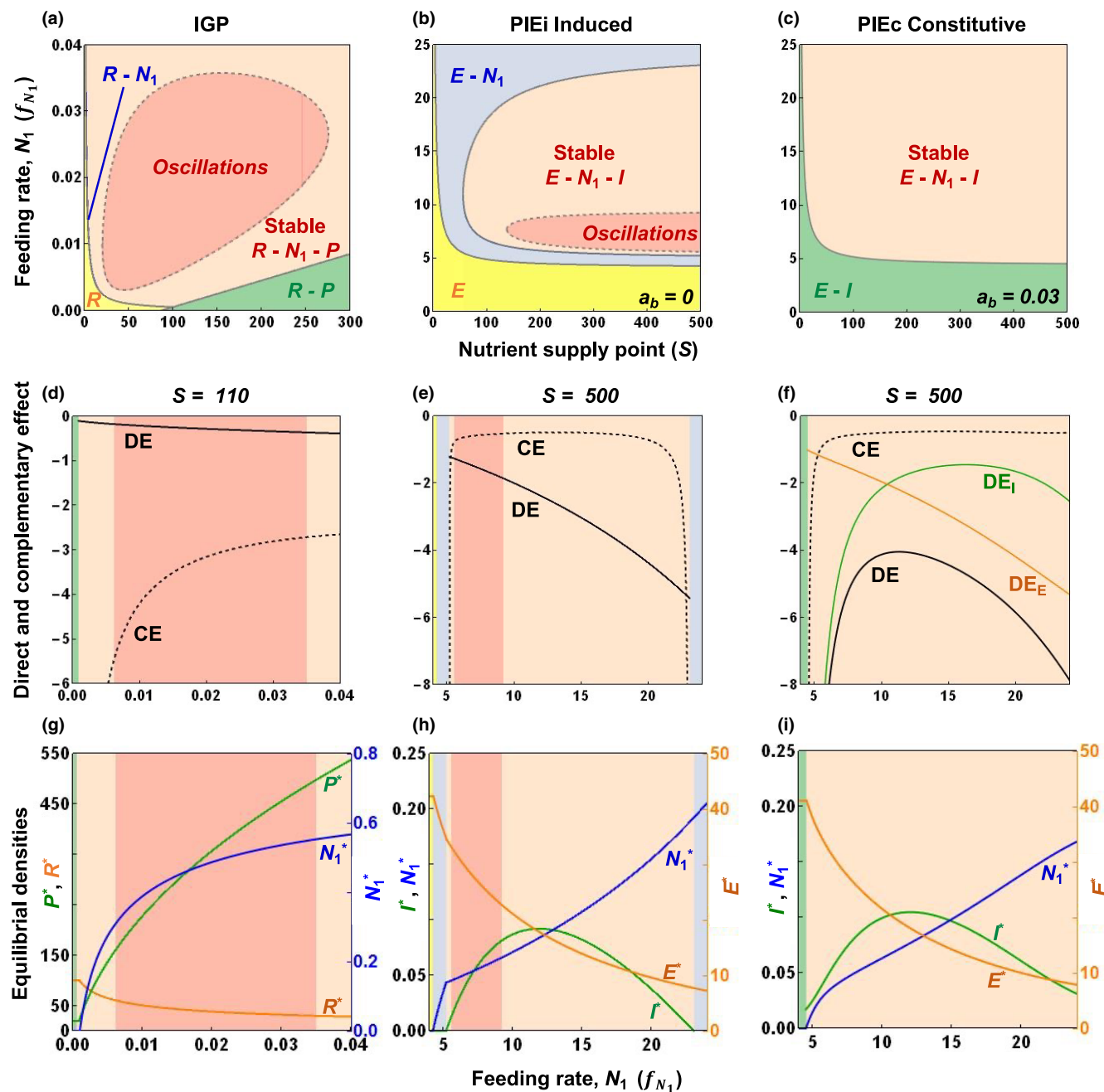


FIGURE 5 Weakening of the product of intraspecific direct and complementary effects generates oscillations in both IGP and PIE models (Figures 2 and 3). (a–c) Bifurcation diagrams over gradients of nutrient supply (S) and feeding rate of prey or parasite (f_{N_1}): Oscillations (dark orange region) found in (a) IGP also arise in the (b) PIEi model of within-host dynamics (see S2). These oscillatory regions are enveloped within a region of stable coexistence (light orange). (c) In PIEc, allocation of baseline energy to immune cells ($a_b > 0$) can eliminate oscillations. (d–f) Direct and complementary effects (after Figure 4): Oscillations occur with weakening of the product of intraspecific direct effects (DE) and intraspecific complementary effects (CE). Weakening of CE primarily triggers oscillations at low f_{N_1} while strengthening of DE restores stability at higher f_{N_1} in (d) IGP and (e) PIEi. In (f) PIEc, self-limitation comes from energy (DE_E , orange) and immune cells (DE_I , green). Stronger DE can eliminate oscillations while lowering parasite burden relative to PIEi (see also Figure A2). (g–i) Equilibrium densities along f_{N_1} : resource, R^* or energy, E^* (orange); prey or parasite, N_1^* , (blue); and predator, P^* or immune cells, I^* (green) in (g) IGP, (h) PIEi and (i) PIEc models. Shifts in these densities weakens or strengthens DE and CE (see text and S2 for details; Table A1 for default parameters).

rates of parasites, the $E - N_1 - I$ remains stable (light orange) or oscillates (only at low a_b). Thus, in PIEc, immune biology eliminates even more states; only $E - I$ and $E - I - N_1$ (oscillations and stable coexistence) remain possible (Figure 5c; refer S2C).

Dynamics—Genesis of oscillations (Figures 1a, 5)
 Despite these differences, oscillations arise for similar reasons in the food web (IGP) and within-host (PIEi, PIEc) models (Figures 1a, 5). As noted (Figure 3; S1), oscillations require weakening of the joint product of

intraspecific direct effects (DE) and complementary effects (CE). In all three cases, stable coexistence ($DE \times CE > 1$) envelopes oscillatory regions ($DE \times CE < 1$; **Figures 5a,b, A3; S2**). In IGP, weakening of CE (less negative) at low feeding rate of the prey, f_{N_1} , triggered oscillations despite strengthening of DE (more negative; **Figure 5d**). At high f_{N_1} , DE strengthens to regain stability. This pattern with CE and DE also arises with increasing feeding rate of parasites in the PIE models (**Figure 5e,f**). The reason behind increasing DE is simpler to understand, as it differed only slightly among models (**Figure 5d-f**, black, solid lines), where DE is:

$$\text{for IGP: } J_{RR} = -a - (f_{N_1} Q_{N_1} N_1^* + f_{PR} Q_P P^*) \quad (2A)$$

$$\text{for PIEi: } J_{EE} = -r - (f_{N_1} N_1^* + e_{IN_1} f_{IN_1} N_1^* I^*) \quad (2B)$$

$$\text{for PIEc: } \underbrace{-r - (f_{N_1} N_1^* + e_{IN_1} f_{IN_1} N_1^* I^*) - a_b}_{\substack{DE_E \\ + \frac{-e_I m_I + e_{IN_1} f_{IN_1} N_1^* E^*}{e_I}}} \quad (2C)$$

In IGP, the additive increase in predator and prey densities strengthens DE of resources (where $DE_R = J_{RR}$; **Equation 2A; S2A**). Thus, strengthening of DE restores stability at higher f_{N_1} (**Figure 5d**, black, solid line). In the PIE models, however, increase in the (weighted) sum of parasites plus the product of parasite and immune cells strengthens DE of energy at higher f_{N_1} (where $DE_E = J_{EE}$; **Equation 2B,C**; **Figure 5e,f**, black, solid line; **S2B**). In all cases, strong enough DE tips an oscillating coexistence equilibrium to stability.

Constitutive immunity enhanced stability in PIEc models by creating immune self-limitation. This self-limitation generates additional loops featured in intra-specific direct (DE) and complementary effects (CE; **Figure 4**). DE now has components from energy (DE_E) and immune cells (DE_I ; **Equation 2C**). The updated DE_E adds fixed energy allocation towards baseline immunity ($-a_b$; **Figure 5f**, orange, solid line). DE_I is always negative too (refer **S2C**). This added immune self-limitation (**Figure 5f**, green, solid line) further strengthens DE (as shown in **Figure 5e**: black, solid line), potentially enough to help to eliminate oscillations in PIEc entirely (**Figure 5c, A3; S2C**). Constitutive immunity also elevates immune cells (I^*), lowering parasite burden (N_1^*) while maintaining slightly higher energy for metabolic work (at rE^* ; **Figures 5h,i**). Hence, constitutive immunity in PIEc stabilized dynamics via self-limitation (**Figure 4**) and reduced parasite burden.

At low feeding rate in both IGP and PIE models, weakening of CE of the prey or parasite triggers oscillations. To understand, recall that CE is a ratio of shorter,

binary loops (F_2) and longer, three-species loops (F_3) (**Figure 3**). In all three models, F_3 became more negative with feeding rate of the prey/parasite, f_{N_1} , than did F_2 (as parameterised). That difference explains why the ratio F_2/F_3 became less negative with increasing f_{N_1} —thereby triggering oscillations (**Figures 4, 5d-f**). Unfortunately, precise details varied among models (preventing further generalisation here).

Dose—Positive feedback leads to priority effects in IGP but not PIE (Figures 1b, 6; S2)

Despite the parallels described above, IGP model can also produce priority effects not found in the within-host analogues (**Figures 1b, 6; S2**). In fact, using different parameter values (**Figure 6a; S2A**), a 2D bifurcation diagram shows two forms of priority effects (PE) in IGP (**Figure 6a**; PE -1 [dark grey] and PE -2 [light grey]). Positive feedback leads to priority effects ensuing positive complementary effects ($CE > 0$) in both forms (**Figure A2**). In these regions, initial densities of species determine competitive outcomes (**Figure 6c,d**). The simpler form of priority effects (PE-1; **Figure 6c**) yields just the prey ($R-N_1$) or just the predator ($R-P$) with the resource. If it held in the PIE models, analogous outcomes would lead to exclusion of immune cells by parasites (yielding stable infection in the $E-N_1$ state) or vice versa (yielding immune clearance, a stable $E-I$), depending on initial parasite dose (**Figure 6e**). However, in PIEi (induced immunity), the host cannot generate immune cells without parasites. Consequently, since the $E-I$ state is both biologically and mathematically not feasible (**S2B**), the analogy breaks. In the other type of priority effects in IGP (PE -2 ; **Figure 6d**), we found either coexistence ($R-N_1-P$) or a predator-only ($R-P$) equilibrium, depending on initial conditions (due to two feasible interior equilibria, one of which is a saddle). Such outcomes would resemble a host that became infected ($E-N_1-I$) or cleared infection ($E-I$), depending on parasite dose (**Figure 6f**). We could not find this outcome in PIEc (**S2C**). Hence, despite the qualitatively similar loop structure, IGP offered two scenarios for priority effects not present in within-host analogues. Alternative infection states would require some other mechanism to produce positive feedback (or $CE > 0$).

Two prey–Predator–resource (KP) | Two parasite–immune - energy (2PIEi / 2PIEc)

Model summary (**Figure 2**; **Table A2; S3**)

Both keystone predation (KP) and within-host (2PIE) models feature two competitors engaged indirectly via consumer-resource-like interactions (**Figure 2**; **Table A2; S3**). In KP, predators (P) can consume two prey (N_i), leading to positive interspecific direct effects for the predator and negative effects on prey (**Figure 2d**). The two prey themselves compete for a shared resource (R), creating similar $+/ -$ interactions. Additionally, the resource

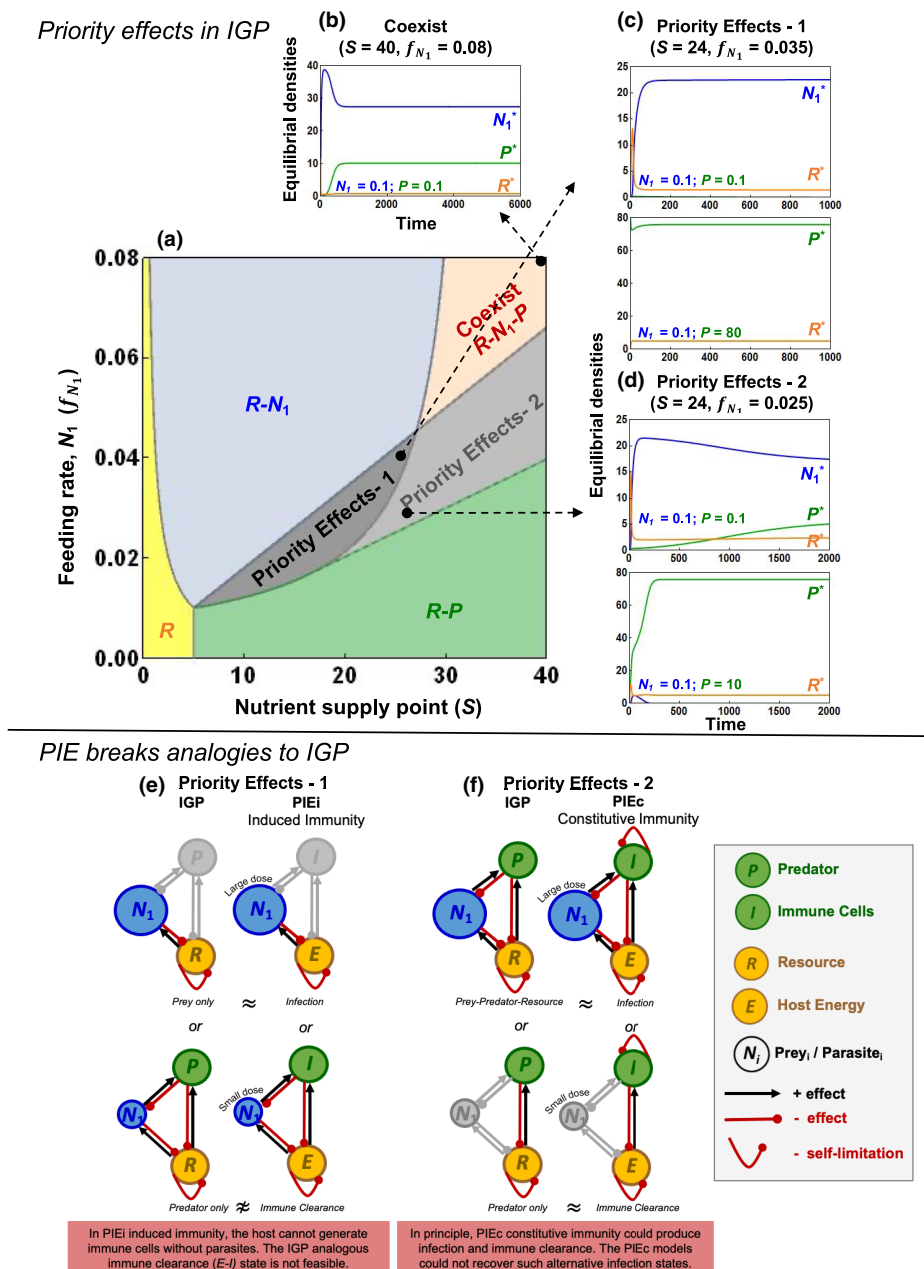


FIGURE 6 Positive intraspecific complementary feedback leads to two forms of priority effects (priority effects-1 and -2) in the IGP model of prey (N_1), predators (P) and resources (R) not found in PIE models. (a) A bifurcation diagram over gradients of nutrient supply point (S) and prey feeding rate (f_{N_1}) and species dynamics at the interior equilibrium (see Figure A2 for more details). (b–d) Sample dynamics. (e, f) PIE models break analogies to IGP. (a, b) Stable coexistence ($R - N_1 - P$, light orange) found in IGP also arises in PIE predicting successful infection (Figure 4; $E - N_1 - I$). (c, d) IGP predicts two forms of priority effects. (a, c, e) In more typical priority effects (priority effects-1; dark grey), either prey ($R-N_1$) or predator ($R-P$) wins. The analogy would lead to infection at large dose ($E-N_1$) or clearance at small dose ($E-I$). However, hosts cannot generate immune cells without parasites, breaking the analogy. (a, d, f) In priority effects-2 (light grey), prey and predator either coexistence ($R-N_1-P$) or the predator wins ($R-P$). We could not find this analogy in PIEc (via parameter searches; see text, S2).

experiences self-limitation at the interior (four species) equilibrium (Figure 2d). Unlike in IGP, the predator does not consume the resource (i.e. it is not omnivorous). Hence, competitors engage only in apparent and exploitative competition (with P and R respectively). Like in KP, parasites in the 2PIE models engage in competition for the shared energy resource and apparent competition due to killing by shared immune cells (Figure 2e,f). However, during these attacks, immune cells use host energy to

proliferate (as in PIE models). Hence, 2PIEi/2PIEc combine IGP and KP-like interactions. Additionally, in 2PIEc, hosts directly allocate energy to production of immune cells ($a_b > 0$) creating self-limitation (Figure 2f; Figure S3). Further, $E-I$ links introduce additional components of loops not found in KP (e.g. in F_3 ; Figure 7; Figure S3B). Therefore, KP might seem too simplistic for comparison to 2PIEi/2PIEc. Yet, as we show, feedback loops that determine coexistence versus priority

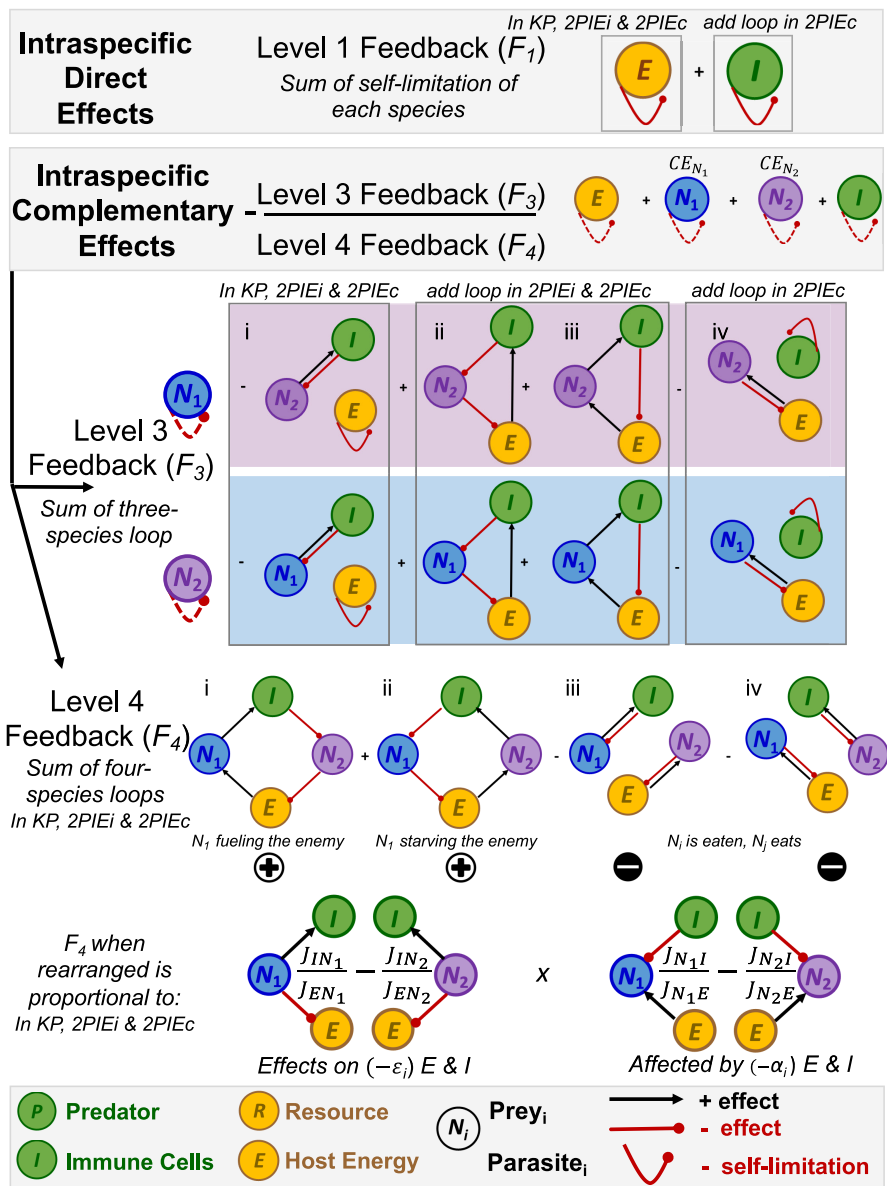


FIGURE 7 Intraspecific direct and complementary effects in four-dimension models: Feedback in KP, 2PIEi and 2PIEc (Figure 2d–f). Evaluated at a feasible interior equilibrium, feedbacks for KP and 2PIEi are nested within 2PIEc. In 2PIEi and 2PIEc, additional loops arise from interactions between immune cells and host energy ('add loop in 2PIEi & 2PIEc'), and immune self-limitation loop ('add loop in 2PIEc'). Level 1 feedback (F_1) sums intraspecific direct effects (solid curves) from energy and immune self-limitation (−; only in 2PIEc). The intraspecific complementary effects (dashed curves) involve a ratio of longer loops, where each species, N_1 (CE_{N_1} ; blue shading) and N_2 (CE_{N_2} ; purple shading), interacts with others in feedback at level 3 (F_3) and 4 (F_4). F_3 sums three-species loops in PIE models: (i) ' N_1 is eaten', the $I-N_1$ loop times E self-limitation (−; all models), (ii) ' N_1 starving the enemy' (+; from PIE models), (iii) ' N_1 fueling the enemy' (−; from PIE models) and (iv) ' N_1 eats', the $E-N_1$ loop times I self-limitation (−; only from 2PIEc). F_4 sums, from $L-R$, two destabilising (+) loops and stabilizing (−) ones. N_i benefits as it is (i) 'fueling' or (ii) 'starving' the enemy (via interspecific competition) but is restrained by (iii) and (iv) ' N_i is eaten, N_j eats' loops (the product of $I-N_i$ and N_j-E loops; intraspecific competition). With some rearrangement, F_4 becomes proportional to differences in ratios of how each competitor has effects on ($-e_i$) and is affected by ($-\alpha_i$) immune cells and host energy (see text). Finally, the sign of F_4 determines that of CE (see text). The predator (P , green), prey 1 (N_1 , blue), prey 2 (N_2 , purple) and resources (R , yellow) in KP are analogous to immune cells (I), parasites (N_1 and N_2) and host energy (E) in 2PIE models respectively.

effects (F_4) of the prey or parasite are qualitatively similar (Figure 7; S3A,B). The resemblance arises because both the prey and parasite are similarly *affected by* and have *effects on* their resources and their enemy. However, stronger negative feedback at level 3 in 2PIEc shrinks opportunities for coexistence while lowering parasite burden (see below).

Intraspecific direct and complementary effects in the 4D KP and 2PIE model (Figure 7)

Similar to 3D systems, the sign of intraspecific complementary effects determines coexistence versus priority effects in 4D systems. But first, in both KP and 2PIEi, only self-limitation of the resource or host energy,

respectively, contributes to summed intraspecific direct effects (DE; level 1 feedback, F_j ; lying on $\text{tr}[\mathbf{J}]$; **Figure 7**; **S3**). 2PIEc has additional contributions from immune self-limitation. Then, summed intraspecific complementary effects (CE) involve a ratio of feedback loops with three species (F_3) and four (F_4 ; $CE = -F_3/F_4$; lying on $\text{tr}[\mathbf{J}^{-1}]$; **Figure 7**; **S3**). In KP and 2PIE models, F_3 sums two $I-N_j$ loops with energy self-limitation (analogous to [i] in PIE [**Figure 4**]). Then, energy-immune interactions add two sets of additional loops, analogous to positive ‘*starving the enemy*’ and negative ‘*fueling the enemy*’ loops in PIE, but for each parasite (loops [ii] and [iii] respectively). Finally, immune self-limitation in 2PIEc adds two more negative feedback loops (involving $N_i - E$ for each parasite; loops [iv]). When those loops are aggregated together, the numerator of the intraspecific complementary effect of N_1 is feedback of the $I-E-N_2$ subsystem (CE_{N_1} ; blue shading), while feedback of the $I-E-N_1$ subsystem provides that of N_2 (CE_{N_2} ; purple shading; **Figure 7**). We find negative F_3 for the interior equilibria evaluated here (algebraically or numerically). Unlike in IGP/ PIE, the intraspecific complementary effect of the enemy and resource now becomes zero. Hence, only the sum of CE_{N_i} determines stability.

Importantly, level 4 feedback loops are qualitatively similar across the KP, 2PIEi and 2PIEc models. These loops (from $L-R$) are: (i) a positive ‘ N_1 fueling the enemy’ loop, where a small increase in one parasite stimulates the immune cells which attack the competing parasite, freeing up energy for the first parasite. In a second positive loop, (ii) ‘ N_1 starving the enemy’, a small increase in a parasite reduces resources, hence density of the competing parasite, thereby lowering immune activation, ultimately reducing mortality on the first parasite. Those two positive (destabilising) loops then push against two negative (stabilising) loops, (iii and iv) ‘ N_i is eaten, N_j eats’. These negative loops therefore add the stabilising consumer-resource interactions within which each prey/parasite is enmeshed. For instance, a small increase in parasite i creates a negative loop with the immune system while parasite j is braked by its loop with the resource. Then, those roles reverse, that is, parasite j is slowed by the immune system and parasite i is by the resource. Summed, those two loops (iii and iv) jointly determine the amount of negative feedback in the system at level 4. Combined then, loops (i)-(iv) determine the sign of the summed complementary indirect effects ($-F_3/F_4$; since $F_3 < 0$: see above) and stability of the interior equilibrium.

In these 4D systems, stability of the interior equilibrium can also be understood via symmetries or asymmetries in two quantities. These quantities emerge upon rearranging the loops comprising the level 4 feedback (F_4). They reflect ratios of how each prey or parasite has effects on ($-\epsilon_i$) and is affected by ($-\alpha_i$) their enemies and resources (**Figure 7**; **Equation 3**; **S3**):

$$F_4 = -J_{N_1 E} J_{N_2 E} J_{E N_1} J_{E N_2} \times \underbrace{\left(\frac{J_{I N_1}}{J_{E N_1}} - \frac{J_{I N_2}}{J_{E N_2}} \right)}_{\text{effects on } (-\epsilon_i)} \times \underbrace{\left(\frac{J_{N_1 I}}{J_{N_1 E}} - \frac{J_{N_2 I}}{J_{N_2 E}} \right)}_{\text{affected by } (-\alpha_i)} \quad (3)$$

where J_{ij} is interspecific direct effects (Jacobian elements) of species j on species i , $\epsilon_1 = -J_{I N_1} / J_{E N_1}$, $\alpha_1 = -J_{N_1 I} / J_{N_1 E}$, etc. Stability hinges on (a)symmetry of these ratios. As described elsewhere (**S3**), the difference in *affected by* ratios ensures a trade-off in traits influencing resource and apparent competition that permits coexistence. If N_1 is the superior resource competitor without the enemy, then $\alpha_1 > \alpha_2$ ensures N_2 is sufficiently resistant to attack. The difference in *effects on* ratios then determines the competitive hierarchies of traits governing exploitative [resource, energy] and apparent [predator, immune] competition. Coexistence occurs with symmetry in these ratios (i.e. if $\alpha_1 > \alpha_2$ if $\epsilon_1 > \epsilon_2$), guaranteeing that net negative feedbacks dominate ($F_4 < 0$). In contrast, asymmetry in these ratios, (e.g. $\alpha_1 > \alpha_2$ still but now $\epsilon_1 < \epsilon_2$) leads to net positive feedback ($F_4 > 0$), triggering priority effects. (These points, and others involving winners of resource and apparent competition, are summarised in Table **A3**, following **S3**).

Coexistence (coinfection) and priority effects in KP and 2PIE (**Figure 8**; **S3**)

Assembly of the interior equilibrium

Despite differences in biology, KP and 2PIEi models share similar four-species feedback loops, hence qualitatively similar outcomes for stability of the interior equilibrium (**Figure 8**; **S3**). That similarity becomes readily apparent in 2D bifurcation diagrams for each model in parameter space of nutrient supply (S) and N_1 ’s feeding rate on resources (f_{N_1}). In KP (A), at low $S - f_{N_1}$, only the resource is supported in the system (R , yellow). Increased feeding rate at low nutrient supply enables prey N_1 to meet its minimum resource requirement ($R-N_1$; light blue). As S increases, their minimum prey requirement is met (its N_1^*), allowing predators to invade ($R-N_1-P$; dark blue). Then, the more resistant N_2 can invade when the $R-N_1-P$ food chain provides enough resources, given predator density (mortality). This invasion enables four-species coexistence ($R-N_1-N_2-P$; light orange). Similar assembly rules apply for invasion of N_2 when feeding rate of N_1 stays low enough to grant N_2 competitive superiority ($R_2^* < R_1^*$). With increasing S , first N_2 invades ($R-N_2$ space; light purple), then the predator does ($R-N_2-P$; dark purple). A less typical assembly arises at lower S ($S = 1$) but with increasing f_{N_1} . Here, N_1 and P simultaneously invade creating the jump from 2 ($R-N_2$) to 4 ($R-N_1-N_2-P$)-dimensional stability (see **S3C**). Overall, similar transitions appear in 2PIE models. Like KP, the possible states

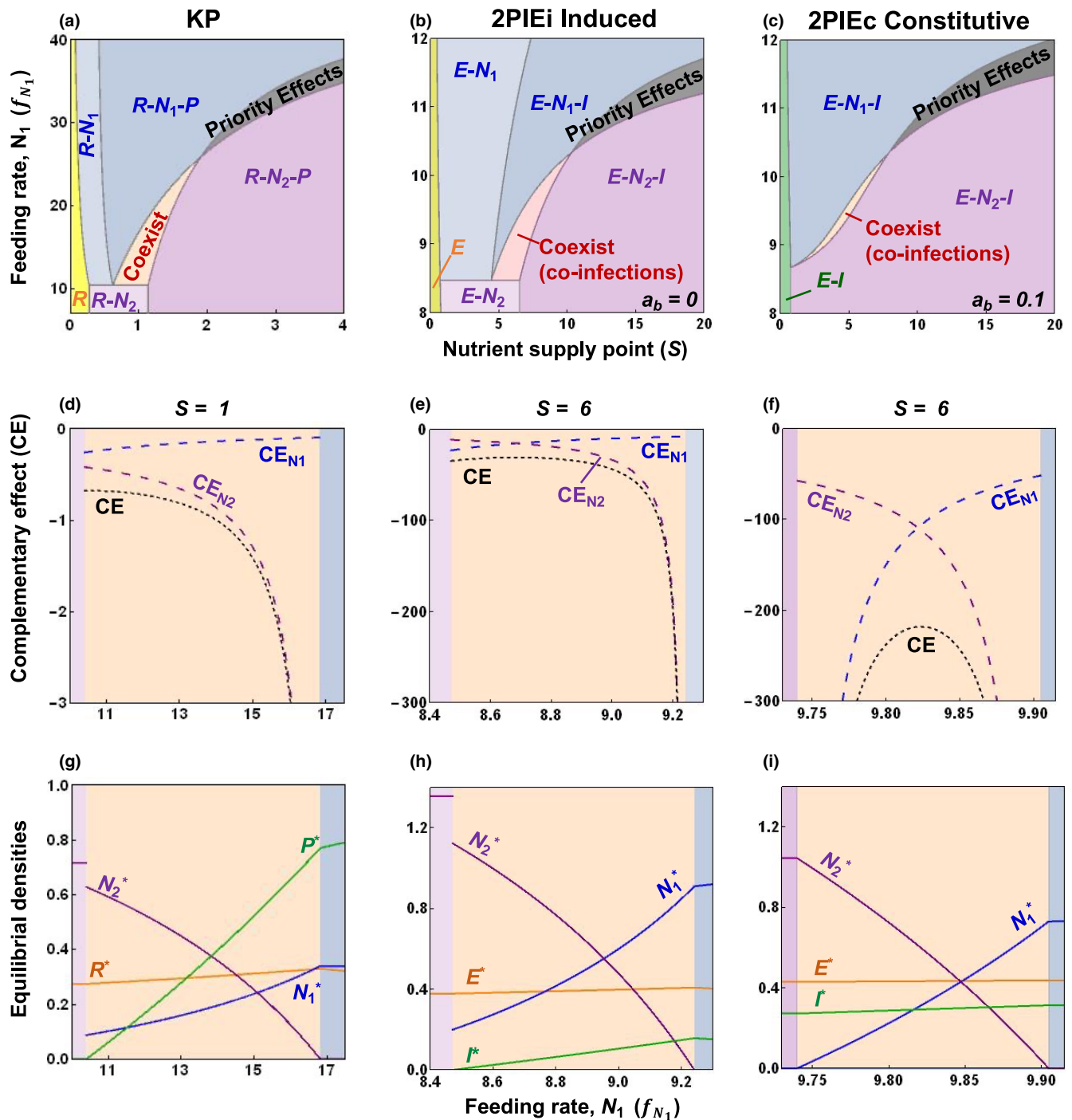


FIGURE 8 KP anticipates coexistence and priority effects in 2PIE models (Figures 2 and 7). (a–c). Bifurcation diagrams over gradients of nutrient supply point (S) and feeding rate of prey or parasite (f_{N_i}): priority effects (grey region) and stable coexistence (orange) found in (a) KP also arise in (b) 2PIEi-induced immunity and (c) 2PIEc constitutive immunity models of within-host dynamics (where $a_b > 0$ denotes baseline energy allocated to immune cells). Stable coexistence (coinfection) happens at low f_{N_i} and S in all three models. (d–f) Complementary effects through coexistence/coinfection regions: Strong, negative complementary effects (CE; black, short dash) from N_1 (CE_{N_1} ; blue, long dash) and N_2 (CE_{N_2} ; purple, long dash) shift systems from coexistence to exclusion of N_1 or N_2 at lower or higher f_{N_i} , respectively, in (d) KP, (e) 2PIEi and (f) 2PIEc. In 2PIEc, the addition of immune self-limitation enhances negative complementary effects and squeezes parameter space enabling coinfection. (g)–(i) Equilibrium densities along f_{N_i} : Resource, R or energy, E (orange); prey or parasite 1, N_1 , (blue); prey or parasite 2, N_2 , (purple); and predator, P or immune cells, I (green) in (g) KP, (h) 2PIEi and (i) 2PIEc models (see text and S3 for details, Table A2 for default parameters).

in 2PIEi models are energy alone (E), just one parasite ($E-N_i$), addition of immune cells ($E-N_i-I$) or an interior equilibrium ($E-N_1-N_2-I$; Figure 8B). However, since hosts

allocate energy to immune cells, they are always present in 2PIEc. Hence, 2PIEc only has $E-I$, $E-I-N_i$ and $E-N_1-N_2-I$ states (but not E or $E-N_i$; Figure 8c).

Diversity—Coinfection versus priority effects

([Figures 1c, 8](#))

In all three models, low or high combinations of nutrient supply point (S) and feeding rate (f_{N_i}) create (a)symmetry in *effects on* and *affected by* ratios that, in turn, generate coexistence or priority effects for a feasible interior equilibrium ([Figures 1c, 8](#)). We assume N_1 competes superiorly for energy without immune cells but is sufficiently more vulnerable to immune attack (enabling $\alpha_1 > \alpha_2$). In the coexistence region (i.e. at lower $f_{N_1} - S$), N_1 is the superior apparent competitor while more resistant N_2 is the superior resource competitor (see [S3A–B](#)). Such a switch in competitive hierarchy means N_1 exerts stronger effects on immune cells relative to energy ($\varepsilon_1 > \varepsilon_2$; [Equation 3](#)). It also produces a symmetry in ratios that generates net negative feedback ($F_4 < 0$) and negative intraspecific complementary effects of the competitors ($CE_i < 0$) enabling coexistence (coinfection; [Figure 8d–f](#)). However, high $f_{N_1} - S$ produces an asymmetry: N_2 now is the superior apparent competitor, and it has stronger effects on immune cells relative to energy ($\varepsilon_1 < \varepsilon_2$) while N_1 is the superior resource competitor. This asymmetry in ratios generates net positive feedback ($F_4 > 0$) triggering priority effects ([S3A, B](#)). Hence, this interior saddle equilibrium separates dominance by one or the other parasite (or prey). Furthermore, intraspecific complementary effects are both positive ($CE_{N_i} > 0$): each competitor now benefits itself through the feedback loops. With even higher f_{N_1} , N_2 becomes excluded in all three models ([Figure 8g–i](#)). The 2PIEc model modifies the predictions of 2PIEi in two ways. Qualitatively, the range of outcomes in $S - f_{N_1}$ space simplifies (as in the PIE models; [Figure 6c](#)). Since baseline allocation guarantees positive density of immune cells, E or $E - N_i$ regions no longer exist ([Figure 8b](#) vs [8c](#)). Quantitatively, in the coinfection region, constitutive immunity strengthens intraspecific complementary effects (because of added negative feedback in F_3 loops, the numerator of CE of each species [[Figure 7](#)]). Stronger CE, in turn, narrows the parameter space permitting coexistence. Constitutive immunity also elevates density of immune cells (I^*), lowering parasite burden ($N_1^* + N_2^*$) while maintaining slightly higher E^* (allocated at rE^*) for other metabolic work (compare [Figures 8h](#) vs. [8i](#)). Hence, constitutive immunity adds to F_3 loop structure of 2PIEc ([Figure 7](#)). That addition squeezes coinfection space while reducing parasite load relative to 2PIEi.

DISCUSSION

What within-host feedbacks determine infection outcome? For insights on how parasite dynamics, dose and diversity govern within-host infection, we turn to food webs. Specifically, we compare two classic food web modules, intraguild predation (IGP) and keystone predation (KP), to their within-host analogues (PIE and 2PIE; [Figure 2](#)). On the one hand, the comparison seems apt.

Both prey and parasite consume a shared resource while facing mortality from an enemy (predator or immune cell). On the other hand, predator and immune cells are produced rather differently. For instance, predators can eat only prey or the resource or both (in IGP). In contrast, induced proliferation of immune cells requires both energy and parasites simultaneously. Furthermore, hosts can allocate energy to immunity constitutively (a pipeline uncommon to food webs). Given these similarities and differences, we analyse stability of equilibria produced by each model using feedback loops. In particular, we interpret loops as direct and complementary intraspecific effects, and we show how their sign and strength govern stability outcomes ([Figure 3](#)). We make three points. First, both IGP and PIE systems predict stable coexistence/infection or oscillations due to similar shifts in direct and complementary effects ([Figure 4](#) and [5](#)). Second, that enemy-generation difference eliminates priority effects seen in IGP—the PIE models cannot produce them without inclusion of other mechanisms ([Figure 6](#)). Third, despite the simpler structure of KP, competing prey and parasites coexist (coinfect) or show priority effects for similar reasons ([Figure 7](#) and [8](#)). The outcomes hinge on the sum of similar four-dimensional loops that generate positive and negative feedback. We show how those loops, in turn, translate into parallel symmetries (stabilising) or asymmetries in *effects on* and *affected by* ratios of the two competitors. Overall, food web models offer powerful if imperfect analogies to feedbacks underlying the dynamical repertoire of parasites within hosts.

Loop analysis and complementary effects

Feedback loops enabled biologically meaningful comparisons of the stabilising and destabilising forces in the models analysed here. The traditional niche toolbox (trait trade-off, bifurcations and assembly rules) and loop approach has been previously applied to food webs. However, this combination has not been applied to within-host modules. Similarly, while general theory has linked food web modules to host–parasite systems (Holt & Dobson, [2006](#)) or compartmental models in epidemiology (e.g. SIR models in Lafferty et al., [2015](#)), we outline its connections to within-host modules using a loop approach. By rearranging traditional stability criteria, we unpack the biology of feedback underlying stability ([Figure 3](#); Puccia & Levins, [1991](#); Novak et al., [2016](#)). These loops can involve shorter, direct effects (DE), where increases in intraspecific density leads to self-limitation here (negative feedback). Longer loops involve chains of connected interactions—here, between two (e.g. binary consumer-resource), three or four species. We show that certain ratios of these loops at different feedback levels, in turn, correspond to intraspecific complementary effects (CE, the trace of the inverse Jacobian

matrix; **Figure 3**). Furthermore, we illustrate how negative CE leads to coexistence (stable or oscillatory [in 3D systems]), and positive CE can produce priority effects. In 3D systems, that transition from stability to oscillations involves weakening of DE x CE. Such weakening occurs when feedback at longer loops becomes too strong relative to those at shorter loops. With that framework in mind, the loops then facilitated comparison between structurally similar but biologically disparate food web and within-host modules.

Dynamics: Oscillatory versus stable infection

This loop-based approach revealed that single prey and parasite can persist—stably or via oscillations—with their resource and enemy for similar reasons. Generally speaking, like in IGP, coexistence in PIE requires summed negative intraspecific complementary effects (CE). Like in IGP, weakening of CE ($-F_2/F_3$) triggers oscillations in PIE (due to weakening of F_3 relative to F_2 ; **Figure 4d,e**). Yet, either the sum (IGP), or sum and product (PIE) of victim and enemy densities strengthens intraspecific direct effects (DE). Strong enough DE then tips the coexistence equilibrium from oscillations to stability. These insights provide alternative, intrinsic explanations for oscillatory dynamics seen, for example, in malarial infections (typically modelled as following externally forced circadian rhythms: Smith et al., 2020). Additionally, in PIEi higher feeding rate of parasites or reduced food consumption by hosts can stabilise oscillations (**Figure 5b**). Those oscillations matter because they create boom-bust parasite-immune cycles that can harm hosts (via oxidative damage, cellular senescence, etc.: Costantini & Møller, 2009). However, in hosts with high constitutive immunity (PIEc), the strengthening of DE by immune-self limitation can prevent oscillations, potentially reducing this damage. Additionally, allocation to constitutive immunity can lower parasite burden while maintaining higher energy for other metabolic work.

Dose: Infection versus immune clearance

Despite similarities in loop structure, priority effects emerge in IGP but not PIE models. The reason for this discrepancy hinges on production of the enemies. In principle, when each prey/parasite ‘starves the enemy’ enough, the resulting positive feedback through the three species might trigger priority effects (**Figure 4**). In fact, IGP here produces two types of them (see also Verdy & Amarasekare, 2010). In the simpler, more typical one, either the prey or the predator dominates. In the other form of priority effects, predator and prey coexist or the prey is excluded (**Figure 6a**). If they existed, such priority effects in PIE models might explain why large infectious doses

overwhelm immune clearance, leading to infection (yielding stable $E-N_1$ or $E-N_1-I$ states), while immune systems can clear small doses (in a stable $E-I$ state, as seen in experiments, e.g. Merrill & Cáceres, 2018). Yet, we found no such priority effects in PIE models as formulated (see also Greenspoon et al., 2018). This difference between IGP and PIE arises because immune proliferation requires energy and parasites *simultaneously*, whereas predator reproduction is fueled by resources and prey *independently*. Hence, some other mechanism must generate priority effects within hosts (e.g. effects of parasites on within-host resource supply points: Van Leeuwen et al., 2019). In the future, such mechanisms could be added to the PIE framework. However, they would break straightforward food web analogies emphasised here.

Diversity: Coinfection versus priority effects

In contrast, KP and 2PIE models produced either coexistence or priority effects of competitors for similar reasons. At first glance, such parallels might seem surprising since KP more simply connects species engaged in resource and apparent competition. In contrast, 2PIE has more complex loop structure (via those omnivory-like $I-E$ connections). Despite these structural differences, both models share qualitatively identical four species loops (**Figure 7**). We translated the net sum of those positive and negative loops into differences in *effects on* and *affected by* ratios for each competitor. Those ratios determine successful coinfection versus priority effects. First, either case requires a sufficient trade-off to enable a feasible interior equilibrium. If one species competes superiorly for host energy, the other must better resist immune attack. Such a trade-off anchors a directionality of the *affected by* ratio (immune to energy) between competing parasites. Coinfection (and coexistence), then, requires symmetry: the parasite with greater *affected by* ratio must also have the greater *effects on* ratio (**Figure 7**, Table A3). Those conditions arise when the superior energy competitor without immune cells (lower minimal energy needs) becomes the superior apparent competitor with them (i.e. it supports highest immune density). Meanwhile, the more resistant parasite becomes the best energy competitor. If true, each parasite indirectly inhibits its own growth and facilitates its competitor. Coinfection ensues due to net negative feedback (Griffiths et al., 2015). In contrast, if one parasite always competes superiorly for energy while the superior apparent competitor enjoys resistance, asymmetry in these ratios ensues. That asymmetry means each parasite indirectly facilitates its own growth and slows its competitor, either by ‘fueling the immune cells’ that attack the competitor (freeing up energy), or by ‘starving the immune cells’ via starving the competitor (**Figure 7**). When strong enough, such interactions ensure priority effects (Devevey et al., 2015) via net positive feedbacks.

These new within-host competition models can also guide future coinfection experiments. First, the competition models focus attention on traits and mechanism. Traditional coinfection experiments alter initial densities/order of arrival of parasites within a host (*reviewed in* Karvonen et al., 2019). Then, mechanism is inferred from pattern. Alternatively, with 2PIE-like models, experimenters could directly measure and/or fit key host-parasite traits that produce within-host dynamics. Second, they highlight how multiple niche dimensions govern competitive outcomes within hosts. Some recent empirical studies emphasized immune- (Ezenwa et al., 2010; Halliday et al., 2018) or resource-mediated (Budischak et al., 2018) competition within hosts. Yet, competition along a single niche dimension predicts only competitive exclusion (*sensu stricto*). Instead, measurements of both immune and energetic niche dimensions together (Budischak et al., 2015) could evaluate the range of outcomes in 2PIE. Third, the bifurcation maps here suggest joint manipulation of nutrient supply to hosts and parasite traits (perhaps by using different parasite strains). Such manipulations could then capture an array of outcomes like exclusion *v* coinfection of malarial parasites (de Roode et al., 2005) or increasing parasite burden along a nutrient gradient (Budischak et al., 2015). Finally, our model predicts that allocation to constitutive immunity strengthens complementary effects, squeezing parameter space allowing coinfection and reducing parasite burden. One could test such predictions using strains with immune knockouts (Chen et al., 2005) or host genotypes differing in immune allocation (Fuess et al., 2021).

Future directions and conclusions

This within-host parasite framework could become expanded in the future. First, models could add niche dimensions. For instance, parasites might compete for multiple within-host resources (*reviewed in* Ezenwa, 2021) and/or face multiple immune defences (Fenton & Perkins, 2010). These additional dimensions parallel food webs with multiple resources and predators (Hulot & Loreau, 2006). These niche dimensions might expand conditions promoting coinfection or priority effects. Second, other mechanisms like relative non-linearities (Armstrong & McGehee, 1980), competitive intransitivity (May & Leonard, 1975) or other variation-based mechanisms (Chesson, 2000) may predict successful coexistence in our within-host framework. For example, since PIE can oscillate, two parasites might coexist via oscillations (relative non-linearities). Similarly, multiple parasites competing intransitively for two or more resources might coexist (Huisman & Weissing, 2001). Third, environmental variation could alter key within-host traits (e.g. temperature fluctuations can modulate host immunity and parasite

attack rates [Scharsack et al., 2016]). Such intersections of environment with trait plasticity might enhance opportunities for parasite coinfection (Chesson, 2000). Finally, the direct (DE) versus complementary effect (CE) approach to predicting oscillations may have limits. Perhaps theoreticians can extend it beyond three to four or more dimensions. Together, these expansions would extend mechanistic models of within-host dynamics and produce insight into disease and coexistence alike.

In this study, we gleaned insights for mechanisms of within-host infection dynamics using food web modules and feedback loops. We conceptually unify free living and within-host dynamics via traditional niche toolbox and feedback loops. These tools empower synthetic comparison across structurally similar but biological distinct systems. The loop grammar also delineates biological mechanisms underlying feedbacks. For instance, despite omnivory-like *I-E* connections in coinfection (2PIE) models, competing parasites coinfect (coexist) or show priority effects like in KP. Those outcomes arose because competitors within hosts or in food webs engage in structurally similar resource and apparent competition. Such comparable structure meant that symmetries in *effects on* and *affected by* ratios (involving the enemy and resource) determined stability of competition. Hence, dynamical forces governing stability in food webs can mirror those within hosts. Real-world infection scenarios indeed involve transient dynamics, stochasticity, time delays in stimulation of immune response, pathogen re-exposure *etc*, that may alter within-host dynamics. Yet, niche-based models present a starting point to understand those real-world dynamics. Furthermore, niche-based insights can guide more predictive experiments at the within-host scale which can then be scaled to the population linking within- to between-host dynamics. For instance, fluctuation in nutrient supply to host could shift competitive outcomes within hosts that then alters multi-parasite outbreaks at the population scale (Hite & Cressler, 2018) or even ecosystem nutrient pool (Borer et al., 2021). Hence, further development of resource and immune-explicit frameworks can only enhance predictive insight into individual health and disease outbreaks alike.

AUTHOR CONTRIBUTIONS

AR and SRH conceptualised the paper. AR performed the analyses (lead), generated the figures and wrote the first draft of the manuscript; SRH performed the analyses (support) and wrote the first draft of the appendix. Both authors substantially contributed to subsequent revisions.

ACKNOWLEDGEMENTS

AR was supported by the Department of Biology, IUB and NSF DEB (1655656). We thank F. Bashey-Visser, C.M Lively, members of the Hall lab for their valuable feedback; N. Wale for feedback on Figure 1; and especially M.

Cortez for some help with loops and matrices. AR credits M. Davis and D. Brubeck for musical inspiration.

CONFLICT OF INTEREST

Authors declare no competing interests.

PEER REVIEW

The peer review history for this article is available at <https://publons.com/publon/10.1111/ele.14142>.

OPEN RESEARCH BADGES



This article has earned Open Materials and Preregistered Research Design badges. Materials and the preregistered design and analysis plan are available at: <https://doi.org/10.5281/zenodo.6570624>.

DATA AVAILABILITY STATEMENT

The code to reproduce all the analysis are available on <https://doi.org/10.5281/zenodo.6570624>

ORCID

Ashwini Ramesh  <https://orcid.org/0000-0003-1629-7024>

REFERENCES

Alizon, S. & van Baalen, M. (2008) Multiple infections, immune dynamics, and the evolution of virulence. *The American Naturalist*, 172(4), E150–E168.

Armstrong, R.A. & McGehee, R. (1980) Competitive exclusion. *The American Naturalist*, 115(2), 151–170.

Bashey, F. (2015) Within-host competitive interactions as a mechanism for the maintenance of parasite diversity. *Philosophical Transactions of the Royal Society B: Biological Sciences*, 370(1675), 20140301.

Borer, E.T., Asik, L., Everett, R.A., Frenken, T., Gonzalez, A.L., Paseka, R.E. et al. (2021) Elements of disease in a changing world: modelling feedbacks between infectious disease and ecosystems. *Ecology Letters*, 24(1), 6–19.

Budischak, S.A., Sakamoto, K., Megow, L.C., Cummings, K.R., Urban, J.F., Jr. & Ezenwa, V.O. (2015) Resource limitation alters the consequences of co-infection for both hosts and parasites. *International Journal for Parasitology*, 45(7), 455–463.

Budischak, S.A., Wiria, A.E., Hamid, F., Wammes, L.J., Kaisar, M.M., van Lieshout, L. et al. (2018) Competing for blood: the ecology of parasite resource competition in human malaria–helminth co-infections. *Ecology Letters*, 21(4), 536–545.

Chen, C.C., Louie, S., McCormick, B., Walker, W.A. & Shi, H.N. (2005) Concurrent infection with an intestinal helminth parasite impairs host resistance to enteric *Citrobacter rodentium* and enhances *Citrobacter*-induced colitis in mice. *Infection and Immunity*, 73(9), 5468–5481.

Chesson, P. (2000) Mechanisms of maintenance of species diversity. *Annual Review of Ecology and Systematics*, 31(1), 343–366.

Costantini, D. & Möller, A.P. (2009) Does immune response cause oxidative stress in birds? A meta-analysis. *Comparative Biochemistry and Physiology Part A: Molecular & Integrative Physiology*, 153(3), 339–344.

Cressler, C.E., Nelson, W.A., Day, T. & McCauley, E. (2014) Disentangling the interaction among host resources, the immune system and pathogens. *Ecology Letters*, 17(3), 284–293.

de Roode, J.C., Helinski, M.E., Anwar, M.A. & Read, A.F. (2005) Dynamics of multiple infection and within-host competition in genetically diverse malaria infections. *The American Naturalist*, 166(5), 531–542.

Devevey, G., Dang, T., Graves, C.J., Murray, S. & Brisson, D. (2015) First arrived takes all: inhibitory priority effects dominate competition between co-infecting *borrelia burgdorferi* strains. *BMC Microbiology*, 15(1), 1–9.

Duneau, D., Ferdy, J.B., Revah, J., Kondolf, H., Ortiz, G.A., Lazzaro, B.P. et al. (2017) Stochastic variation in the initial phase of bacterial infection predicts the probability of survival in *D. melanogaster*. *eLife*, 6, e28298.

Ezenwa, V.O. (2021) Co-infection and nutrition: integrating ecological and epidemiological perspectives. In: *Nutrition and infectious diseases*. Cham: Humana, pp. 411–428.

Ezenwa, V.O., Etienne, R.S., Luikart, G., Beja-Pereira, A. & Jolles, A.E. (2010) Hidden consequences of living in a wormy world: nematode-induced immune suppression facilitates tuberculosis invasion in African buffalo. *The American Naturalist*, 176(5), 613–624.

Ezenwa, V.O. & Jolles, A.E. (2011) From host immunity to pathogen invasion: the effects of helminth coinfection on the dynamics of microparasites. *Integrative and Comparative Biology*, 51(4), 540–551.

Fellous, S. & Koella, J.C. (2009) Infectious dose affects the outcome of the within-host competition between parasites. *The American Naturalist*, 173(6), E177–E184.

Fenton, A. & Perkins, S.E. (2010) Applying predator-prey theory to modelling immune-mediated, within-host interspecific parasite interactions. *Parasitology*, 137(6), 1027–1038.

Fuess, L.E., Weber, J.N., den Haan, S., Steinle, N.C., Shim, K.C. & Bolnick, D.I. (2021) Between-population differences in constitutive and infection-induced gene expression in threespine stickleback. *Molecular Ecology*, 30(24), 6791–6805.

Gorsich, E.E., Etienne, R.S., Medlock, J., Beechler, B.R., Spaan, J.M., Spaan, R.S. et al. (2018) Opposite outcomes of coinfection at individual and population scales. *Proceedings of the National Academy of Sciences*, 115(29), 7545–7550.

Graham, A.L. (2008) Ecological rules governing helminth-microparasite coinfection. *Proceedings of the National Academy of Sciences*, 105(2), 566–570.

Greenspoon, P.B., Banton, S. & Mideo, N. (2018) Immune system handling time may alter the outcome of competition between pathogens and the immune system. *Journal of Theoretical Biology*, 447, 25–31.

Griffiths, E.C., Fairlie-Clarke, K., Allen, J.E., Metcalf, C.J.E. & Graham, A.L. (2015) Bottom-up regulation of malaria population dynamics in mice co-infected with lung-migratory nematodes. *Ecology Letters*, 18(12), 1387–1396.

Griffiths, E.C., Pedersen, A.B., Fenton, A. & Petchey, O.L. (2014) Analysis of a summary network of co-infection in humans reveals that parasites interact most via shared resources. *Proceedings of the Royal Society B: Biological Sciences*, 281(1782), 20132286.

Halliday, F.W., Umbanhowar, J. & Mitchell, C.E. (2018) A host immune hormone modifies parasite species interactions and epidemics: insights from a field manipulation. *Proceedings of the Royal Society B*, 285(1890), 20182075.

Hite, J.L. & Cressler, C.E. (2018) Resource-driven changes to host population stability alter the evolution of virulence and transmission. *Philosophical Transactions of the Royal Society B: Biological Sciences*, 373(1745), 20170087.

Holt, R.D. & Dobson, A.P. (2006) Extending the principles of community ecology to address the epidemiology of host-pathogen systems. *Disease ecology: community structure and pathogen dynamics*, 1, 6.

Holt, R.D., Grover, J. & Tilman, D. (1994) Simple rules for interspecific dominance in systems with exploitative and apparent competition. *The American Naturalist*, 144(5), 741–771.

Holt, R.D. & Polis, G.A. (1997) A theoretical framework for intraguild predation. *The American Naturalist*, 149(4), 745–764.

Huisman, J. & Weissing, F.J. (2001) Fundamental unpredictability in multispecies competition. *The American Naturalist*, 157(5), 488–494.

Hulot, F.D. & Loreau, M. (2006) Nutrient-limited food webs with up to three trophic levels: feasibility, stability, assembly rules, and effects of nutrient enrichment. *Theoretical Population Biology*, 69(1), 48–66.

Hurwitz, A. (1895) On the conditions under which an equation has only roots with negative real parts. *Mathematische Annalen*, 46, 273–284.

Karvonen, A., Jokela, J. & Laine, A.L. (2019) Importance of sequence and timing in parasite coinfections. *Trends in Parasitology*, 35(2), 109–118.

Koelle, K., Farrell, A.P., Brooke, C.B. & Ke, R. (2019) Within-host infectious disease models accommodating cellular coinfection, with an application to influenza. *Virus Evolution*, 5(2), vez018.

Lafferty, K.D., DeLeo, G., Briggs, C.J., Dobson, A.P., Gross, T. & Kuris, A.M. (2015) A general consumer-resource population model. *Science*, 349(6250), 854–857.

Leibold, M.A. (1996) A graphical model of keystone predators in food webs: trophic regulation of abundance, incidence, and diversity patterns in communities. *The American Naturalist*, 147(5), 784–812.

May, R.M. & Leonard, W.J. (1975) Nonlinear aspects of competition between three species. *SIAM Journal on Applied Mathematics*, 29(2), 243–253.

Merrill, T.E.S. & Cáceres, C.E. (2018) Within-host complexity of a plankton-parasite interaction. *Ecology*, 99(12), 2864–2867.

Metcalf, C.J.E., Grenfell, B.T. & Graham, A.L. (2020) Disentangling the dynamical underpinnings of differences in SARS-CoV-2 pathology using within-host ecological models. *PLoS Pathogens*, 16(12), e1009105.

Mideo, N., Alizon, S. & Day, T. (2008) Linking within-and between-host dynamics in the evolutionary epidemiology of infectious diseases. *Trends in Ecology & Evolution*, 23(9), 511–517.

Novak, M., Yeakel, J.D., Noble, A.E., Doak, D.F., Emmerson, M., Estes, J.A. et al. (2016) Characterizing species interactions to understand press perturbations: what is the community matrix? *Annual Review of Ecology, Evolution, and Systematics*, 47, 409–432.

Otterstatter, M.C. & Thomson, J.D. (2006) Within-host dynamics of an intestinal pathogen of bumble bees. *Parasitology*, 133(6), 749–761.

Pawelek, K.A., Huynh, G.T., Quinlivan, M., Cullinane, A., Rong, L. & Perelson, A.S. (2012) Modeling within-host dynamics of influenza virus infection including immune responses. *PLoS Computational Biology*, 8(6), e100258.

Puccia, C.J. & Levins, R. (1991) Qualitative modeling in ecology: loop analysis, signed digraphs, and time averaging. In: *Qualitative simulation modeling and analysis*. New York, NY: Springer, pp. 119–143.

Routh, E.J. (1877) A treatise on the stability of a given state of motion, particularly steady motion: being the essay to which the Adams prize was adjudged in 1877, in the University of Cambridge. Macmillan and Company.

Schärack, J.P., Franke, F., Erin, N.I., Kuske, A., Büscher, J., Stolz, H. et al. (2016) Effects of environmental variation on host-parasite interaction in three-spined sticklebacks (*Gasterosteus aculeatus*). *Zoology*, 119(4), 375–383.

Smith, L.M., Motta, F.C., Chopra, G., Moch, J.K., Nerem, R.R., Cummins, B. et al. (2020) An intrinsic oscillator drives the blood stage cycle of the malaria parasite *Plasmodium falciparum*. *Science*, 368(6492), 754–759.

Van Leeuwen, A., Budischak, S.A., Graham, A.L. & Cressler, C.E. (2019) Parasite resource manipulation drives bimodal variation in infection duration. *Proceedings of the Royal Society B*, 286(1902), 20190456.

Verdy, A. & Amarasekare, P. (2010) Alternative stable states in communities with intraguild predation. *Journal of Theoretical Biology*, 262(1), 116–128.

Vogels, C.B.F., Rückert, C., Cavany, S.M., Alex Perkins, T., Ebel, G.D. & Grubaugh, N.D. (2019) Arbovirus coinfection and co-transmission: a neglected public health concern? *PLoS Biology*, 17(1), e3000130.

Wodarz, D. (2006) Ecological and evolutionary principles in immunology. *Ecology Letters*, 9(6), 694–705.

SUPPORTING INFORMATION

Additional supporting information can be found online in the Supporting Information section at the end of this article.

How to cite this article: Ramesh, A. & Hall, S.R. (2023) Niche theory for within-host parasite dynamics: Analogies to food web modules via feedback loops. *Ecology Letters*, 00, 1–18.
Available from: <https://doi.org/10.1111/ele.14142>